



Research article

Jellyfish search algorithm for optimization operation of hybrid pumped storage-wind-thermal-solar photovoltaic systems

Phu Trieu Ha^a, Bach Hoang Dinh^{a,*}, Tan Minh Phan^b, Thang Trung Nguyen^b

^a Faculty of Electrical and Electronics Engineering, Ton Duc Thang University, Ho Chi Minh City, Vietnam

^b Power System Optimization Research Group, Faculty of Electrical and Electronics Engineering, Ton Duc Thang University, Ho Chi Minh City, Vietnam

ARTICLE INFO

Keywords:

Electric generation cost
Generating mode
Pumping mode
Fuel cost reduction

ABSTRACT

This study applies Jellyfish Search Algorithm and five other algorithms to minimize the electricity generation cost of two hybrid systems for one operating day. The first system comprises one pumped storage hydroelectric plant and two thermal power plants. The second system is expanded by integrating one wind and one solar photovoltaic power plant into the first system. For each system during one operating day, the pumped storage hydroelectric plant with only generation mode acts as a conventional hydroelectric plant in the first scenario. Still, it can run pumps to store water and produce electricity in the second scenario. As a result, JSA can reach smaller costs than all compared algorithms, from about 1 % to higher than 10 % for two scenarios in the two systems. The comparisons of generation cost indicate the second scenario with the pumped storage hydroelectric plant can reach a smaller cost than the first scenario with the conventional hydroelectric power plant by \$53,359.7, corresponding to 7.4 % in the first system and \$39,472.8, corresponding to 6.95 % in the second system. Therefore, the water storage function of the pumped storage hydroelectric plant is very effective in reducing the electricity generation costs for hybrid power systems.

1. Introduction

Economic and industrial developments worldwide have significantly increased the demand for electricity in the past decades, mainly supplied by fossil-burning process-based thermal power plants [1]. As a result, the high cost of electricity production and the serious greenhouse gas emissions of power systems are big problems in our lives. Thus, various power plants with lower cost, lower emission, or no emission technologies are encouraged to build and replace the THPs in which RPPs based on wind flow and solar radiation are precious solutions [2]. However, the most significant disadvantage of the RPPs is their power output, which is highly dependent on weather conditions and not controllable according to load demand [3]. To solve the big problem of the RPPs, the studies [4–6] proposed the integration of a battery energy storage system (BESS) into a hybrid system based on solar panels (SPs), diesel generators (DGs) and wind turbines (WTs) to reach the minimum net present cost, which is the sum of the capital cost, operation and maintenance cost, replacement cost, and diesel fuel cost. The study [4] designed one hybrid renewable energy system with BESS, SPs, DGs, and WT for a microgrid in Dakhla, Morocco. The influence of solar radiation, wind speed, diesel fuel, and interest rate on the net

* Corresponding author.

E-mail addresses: hatrieuphu.st@tdtu.edu.vn (P.T. Ha), dinhhoangbach@tdtu.edu.vn (B.H. Dinh), phanminhtan@tdtu.edu.vn (T.M. Phan), nguyentrongthang@tdtu.edu.vn (T.T. Nguyen).

<https://doi.org/10.1016/j.heliyon.2024.e29339>

Received 26 April 2023; Received in revised form 8 March 2024; Accepted 5 April 2024

Available online 6 April 2024

2405-8440/© 2024 Published by Elsevier Ltd.

This is an open access article under the CC BY-NC-ND license

(<http://creativecommons.org/licenses/by-nc-nd/4.0/>).

Abbreviations

THP	Thermal power plant
WPP	Wind power plant
SPPP	Solar photovoltaic power plant
PSHEP	Pumped storage hydroelectric plant
RPPs	Renewable power plants
HEPs	Hydroelectric plants
LOM	Lagrange optimization method
EP	Evolutionary Programming
PSO	Particle swarm optimization
GA	Genetic algorithm
SA	Simulated annealing algorithm
MILP	Mixed integer linear programming
DP	Dynamic programming
IA	Iterative algorithm
TTA	Three-step algorithm
AM	Analysis method
TSA	Tunicate swarm algorithm
ASBO	The best and worst members-based algorithm
JSA	Jellyfish search algorithm
NGA	Northern goshawk algorithm
AHA	Artificial hummingbird algorithm
WSOA	War strategy optimization algorithm

Nomenclature

$TP_{t,itv}$	Generation of the t th THP at the itv^{th} interval
$ce_{1t}, ce_{2t}, ce_{3t}$	Coefficients of cost-power function of the t th THP
$GenCost_{tp}$	Total generation cost of all THPs
N_1	Number of THPs
N_2	Number of intervals
N_3, N_4, N_5	Number of WPPs, SPPPs and PSHEPs
$WP_{w,itv}$	Power output of the w th wind power plant at the itv^{th} interval
$PP_{p,itv}$	Power output of the p th photovoltaic power plant at the itv^{th} interval
$HP_{m,itv}, HP_{m,itv}^{pump}$	Power output and pump power of the m th PSHEP at the itv^{th} interval
$P_{Loss_{itv}}, P_{Load_{itv}}$	Power loss and demand of loads at the itv^{th} interval
$TP_{t,s}^{Low}, TP_{t,s}^{Up}$	Lower and upper generation limits of the s th THP
WP_w^{Low}, WP_w^{Up}	Lower and upper generation limits of the w th WPP
PP_p^{Low}, PP_p^{Up}	Lower and upper generation limits of the p th SPPP
HP_m^{Low}, HP_m^{Up}	Lower and upper generation limits of the m th PSHEP
Q_m^{Low}, Q_m^{Up}	Lower and upper discharge limits of the m th PSHEP
V_m^{Low}, V_m^{Up}	Lower and upper volume limits of the m th PSHEP
$V_{m,itv}$	Reservoir volume of the m th PSHEP at the itv^{th} interval
$Ve_{w,itv}$	Wind speed at the itv^{th} interval in the w th WPP
SR_p	Solar radiation corresponding to the standard environment in the p th SPPP (W/m^2)
$SR_{p,itv}$	Solar radiation at the itv^{th} interval in the p th SPPP
CIP_w	Certain irradiance point (W/m^2)
S_i	The i th solution in the whole population
LoB, UpB	Lower and the upper boundaries of all decision variables
ω_i	Random matrix with terms within 0 and 1 for the i th solution
N_{PZ}	Population size
rdn	Random value between 0 and 1
FS_i^{new}, FS_i	New and old fitness value of the i th jellyfish

present cost and levelized energy cost was considered. The impact of scale variation on power supply probability loss was clarified. The study reached the best results for the net present cost and energy's levelized cost of \$74,327 and 0.0917/kWh, respectively. The study [5] designed two hybrid renewable energy systems for a microgrid in El Kharga Oasis, Egypt. The first system comprised BESS, SPs, WTs, and DGs, whereas the second neglected WTs. As a result, the first hybrid renewable energy system's cost was 286,874 \$,

equivalent to an energy cost of 0.2309 \$/kWh, but the second system's cost was 322,674 \$, equivalent to an energy cost of 0.2597 \$/kWh. The study [6] designed three hybrid renewable energy systems for a microgrid in the Farafra region of Egypt. The study [6] considered all components, including BESS, SPs, DGs, and WTs for the first system; however, it neglected WTs for the second system and SPs for the third system. As a result, the first system could reach the best results with the best net present cost of \$187,181, corresponding to energy's levelized cost of 0.213 \$/kWh. The total cost and energy cost were \$214,530 and 0.2452 \$/kWh respectively for the second system and \$603,026 and 1.81 \$/kWh respectively for the third system. The three studies [4–6] indicated that photovoltaics and wind turbines are essential for microgrids with BESS; meanwhile, BESS has played a significant role in using renewable energies the most effectively. For large power systems with thermal power plants, the long start-up time of the fossil-burning process in generating units and the uncertainty of solar radiation and wind speeds become serious impacts on the stability of power systems. Thus, integrating HEPs into the RPPs and THPs-based power systems is urgently necessary.

In the past decades, combining HEPs and TPPs has been widely applied for short-term hydrothermal power systems [7]. Then, those such problems have been expanded by integrating RPPs into hydrothermal power systems such as short-term fixed head wind-hydro-thermal power systems [8], short-term variable head wind-hydro-thermal power systems [9], and solar-wind-hydrothermal power system [10]. The latter problems have the same feature as considering sufficient water in reservoirs for one day or one week, but this assumption is not valid for several dry seasons. A solution to the lack of water is the use of a pumped storage hydroelectric plant (PSHEP), which can use the surplus power of the RPPs effectively at low-demand hours. Fig. 1 below describes the main characteristics and the outperformance of the PSHEPs [11]. As we can see, there are two different water tanks called upper and lower reservoirs in which the lower should normally be smaller. A generator is used to produce electricity when water is discharged from the upper to the lower, and it can also run as a pump to take water from the lower to the upper levels when it is powered by the grid [12]. Thus, the generator can act as a pump to store water at the upper reservoir by using the surplus power of RPPs and producing electricity at high-demand hours, similar to a conventional hydroelectric plant [13].

Of course, the efficiency of PSHEPs is not one hundred percent because pumping water from a low level to a higher level always needs more energy than energy produced by discharging water from higher to lower potential levels. The selection of pump/generation operation modes and the pump/generation power is essential and directly influences the performance of the integrated power systems. A 0.75 efficiency was used for the PSHEP scheduled over six 4-h periods, and this plant had a high contribution to the cost reduction for one THP by applying LOM [14]. Then, the system was replicated in two other studies using EP [15] and PSO [16]. LOM is a deterministic optimization algorithm based on the Lagrange optimization function; meanwhile, EP and PSO depend on randomizations. LOM could reach the most effective solution, satisfying all constraints and reaching the smallest generation cost, whereas EP and PSO could not reach more effective solutions. However, LOM has not been widely applied for large-scale power systems with renewable power plants and a high number of power plants because it remarkably depends on objective function and constraints. On the contrary, high-performance metaheuristic algorithms and numerical methods have been proposed and applied for large-scale benchmark and national power systems. Latter studies have proved the significant contributions of PSHEP to power systems and the potential performance of these algorithms.

Many studies have successfully found optimal operation solutions for national power systems with the PSHEP. Solving the large-scale power systems in Portugal [17], Iran [18], China [19,20], Spain [21], Turkey [22], and Saudi Arabia [23] have reached exciting results regarding technical and economic issues. For a newly constructed small power system in Portugal [17], PSHEP acted as a slack power source to consume the surplus energy from WPP at low-demand hours and compensate for the lack of power from both geothermal and wind power plants at other hours. A stochastic scheduling model was proposed to consider the varying operating conditions and uncertainty of inflows forecast. The reduction of energy loss by 7 % was obtained to be the success of the power system in Portugal. An analysis method based on a power grid's parameters and characteristics of PSHEP was proposed to reach smaller generation costs of thermal power plants for a small power system in Iran [18]. The power grid information was collected and analyzed to decide the operating mode of PSHEP, and then the information and PSHEP's characteristics were used to determine the PSHEP's generation. For a two-year operating period, the total cost was reduced by \$187,586,000 thanks to the operation of PSHEP [18]. Both technical and economic objectives, namely power reliability level and levelized cost of energy, have been simultaneously optimized for a power system in China [19]. A modified PSO was proposed and proved to have more potential than GA and SA. Obtained results have shown that PSHEP could reduce investment costs by about 50 % and 35 % compared to other systems without solar and wind plants. The study [20] considered an integrated power system in China, and it could reach a higher total electricity sales revenue by about 16 % thanks to the operation of the sole PSHEP [20]; however, the study [20] has not shown any methods to reach operating parameters

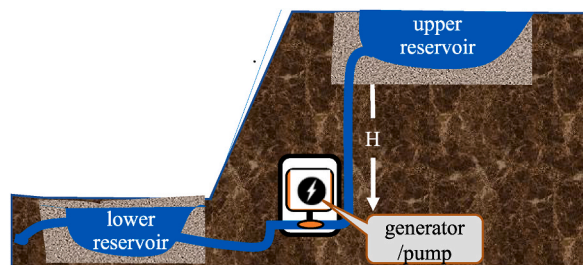


Fig. 1. A typical pumped storage hydroelectric plant.

of power plants, excluding the application of a neural network-based method for predicting generation of solar photovoltaic arrays. MILP method was applied to minimize the total costs of thermal power plants, including fuel, hot start-up, cold start-up, and maintenance costs for an island power system with one PSHEP, WPP, and THP in Spain [21]. MILP has successfully reduced the generation cost of the THP and stabilized the operation of WPP [21]. A power system with one PSHEP and WPP in Turkey was simulated in Ref. [22] using the TTA. A short-term memory network was employed to estimate the electricity prices of the following day in the first step. Then, reanalysis data was utilized to determine available wind power in the second step. Finally, the pump power or generation power of PSHEP was calculated in the last step. After reaching all the parameters of the system, the total sales revenue was calculated, and it increased to about 3.5 % compared to the operation without PSHEP. In the study [23], an integrated power system in Saudi Arabia with one PSHEP and other small power plants could drop about 90 % of diesel generators' total emission volume; however, the study [23] has not presented any methods to reach the generation for the power system.

On the other hand, benchmark power systems with more complicated operational conditions were proposed to demonstrate the effectiveness of optimization algorithms and the benefits of PSHEPs in practical applications [24,25]. In the study [24], an IEEE 24-node transmission network with one PSHEP, one WPP, and ten THPs was tested for different values of pump efficiency of the PSHEP, changing from 0.6 to 0.9. Two assumptions have been adopted for the PSHEP, including fixed speed and variable speed for the pumps of the PSHEP. The results indicated that the one-day revenue of the system with the variable pump speed was always greater than that with fixed pump speed by 8.6 %, thanks to the energy storage of the PSHEP. However, the study has not reported any applied methods for reaching the results. In the study [25], an IEEE 14-node transmission power network with one PSHEP and other power plants such as wind, solar, thermal, and conventional hydroelectric plants has been optimally scheduled to reduce the day-ahead dispatch cost. Three study cases have been tested: decreasing the ramp-up and ramp-down generation, increasing the minimum ramp-up and ramp-down generation, and decreasing the maximum capacity of transmission lines. The day-ahead dispatch cost has been increased to 6.47 %, 7.3 %, and 9.77 % for the three cases, respectively. Two other recent studies have proposed constructing pumping stations separately into the conventional hydroelectric plants, but the conventional hydroelectric plants could work as PSHEPs [26,27]. Pumping stations were constructed between cascaded hydroelectric plants to pump water from downstream to upstream plants [26]. Although the study did not use PSHEPs, water was stored and discharged to produce more power in the upper hydroelectric plant. Open-cast coal mines were left idle once the coal was extracted. The open-cast coal mines have been used as upper reservoirs of PSHEPs to store water [27]. The use of the available open-cast coal mines could reduce the construction costs of the upper reservoir; however, the study neglected the amount of water infiltrating the ground of the open-cast coal mines. The two studies have the same shortcomings of applied algorithms: a very old deterministic algorithm, DP, was applied in Ref. [26], and IA based on characteristics of power plants was proposed in Ref. [27]. The two algorithms cope with several disadvantages that could not be widely and successfully applied, such as low accuracy and time-consuming simulation [28–31].

In general, the mentioned studies have proved significant contributions of PSHEP in various aspects of power system optimal operation, such as reducing the generation cost of TPPs, improving the stabilization of renewable energy sources (WPPs and SPPPs), increasing the total revenue of electricity sales, and reducing investment cost of power systems. However, there were unexpected shortcomings in the studies. They are summarized as follows.

1. The studies have utilized low-performance methods to find design and operation solutions: Conventional metaheuristics coping with local optimal solution low convergence speed, such as MPSO, GA, and SA [19]; Deterministic algorithms with the complex application and time-consuming disadvantages such as MILP [21] and DP [26]; Analysis algorithms based on the characteristic of loads and power plants with the narrow applications and time-consuming disadvantage, such as AM [18], IA [27], and TSM [22]. In addition, no algorithms were presented in Refs. [17,20,23–25].
2. Most previous studies have yet to prove the optimal operation of PSHEPs in storing water and generating electricity. These studies have compared a system without PSHEPs with another system with PSHEPs, which they considered to have a high value of inflows from natural rivers to the upper reservoir of PSHEPs. The high inflows can be used to produce electricity, and the energy generated by the PSHEPs is used to reduce the power from thermal power plants. Indeed, systems without PSHEPs must use more power from thermal power plants, leading to a high cost for the systems. So, the systems with PSHEPs in the previous studies had a high possibility of reaching a smaller cost than those without PSHEPs.
3. The hydraulic constraints of PSHEPs have yet to be demonstrated to be satisfied. The hydraulic constraints in hydropower plants are complicated due to many limiting factors regarding discharge and volume. In addition, the initial and end reservoir volumes are two important constraints. Normally, if the end reservoir volume is much smaller than the initial reservoir value, the stored water is used too much and the system gets the risk of a lack of water in the following periods. Hence, neglecting the constraints cannot show the effective operation of PSHEPs in integrated power systems.
4. Lack of explicit demonstration about the effectiveness of PSHEPs. All studies only performed one PSHEP scenario with pump and generation modes, which have yet to prove the benefits of PSHEP.

These shortcomings are considered and solved in the study. The novelty of the study can be summarized as follows.

1. Consider two cases for the PSHEPs. The PSHEPs perform only generation mode, like conventional hydroelectric plants (CHEPs) in the first case. The second case considers the PSHEPs with either pump mode or generation mode at each period. The initial volume and end volume of the upper reservoir are constrained to be the same in the two cases. The consideration assures that the two power plant types only use inflows from the natural river in [Case 1](#), and both inflows from the river and pumped water in [Case 2](#).

2. Consider specific constraints of PSHEPs regarding the upper reservoir’s discharge, volume limits, and initial and end volumes. Hourly discharge, inflow, and pumped water are employed to draw the hourly volume of the reservoir. Visual descriptions clearly show hydraulic constraints, and the violation or satisfaction of constraints can be seen explicitly.
3. Apply six algorithms, including TSA, ASBO, JSA, NGA, AHA, and WSOA, which were developed in 2020–2022 and presented in Refs. [28–33]. These algorithms have been proven to be powerful for benchmark functions. They were more effective than many popular algorithms, such as Genetic Algorithm, Particle Swarm Optimization, etc., and other previously published algorithms. For example, TSA has been proven to be more effective than Spotted Hyena Optimizer (2017) [34], Grey Wolf Optimizer (2014) [35], Sine Cosine Algorithm (2016) [36], Gravitation Search Algorithm (2009) [37], and Emperor Penguin Optimizer (2018) [38]. Similarly, JSA was compared to PSO, GA, DE, and other previously published algorithms, such as Gravitation Search Algorithm (2009) [37], Whale Optimization Algorithm (2016) [39], Tree-Seed Algorithm (2015) [40], Symbiotic Organisms Search (2014) [41], Teaching-Learning-Based Optimization (2011) [42], Firefly Algorithm (2009) [43], and Artificial Bee Colony (2007) [44].

The contributions of the study can be summarized as follows.

1. Clarify the benefits of PSHEPs in two integrated power systems. Thanks to the water storage function, PSHEPs can generate electricity to cut high power generation from THPs, reducing total electricity generation costs from the plants.
2. Find the most suitable algorithm. Simulation results for the two power systems were found by using six algorithms. Each has been proven to be more effective than about ten others in Refs. [28–33]. However, they could be effective for some problems and ineffective for others. So, in the study, they were run for two power systems with two cases for each. All these algorithms have successfully solved the power systems with valid solutions but different high solution quality. JSA has reached valid solutions with the smallest total generation costs among these six algorithms. So, JSA is the most suitable algorithm among the six algorithms.
3. Find the most suitable algorithm for two considered power systems, which can find the most optimal solutions for power systems with the operation of PSHEPs.
4. Reach the smallest total generation cost of thermal power plants to maximize economic benefits for integrated power systems.

2. Problem formulation

2.1. Objective function

The generation and electricity generation fuel cost characteristic of a typical THP plotted in Fig. 2 indicates the generation of THPs directly influences the economic effectiveness of power systems. So, determining the suitable generation values for the plants is a significant task to pay the lowest cost, and using PSHEPs to reach the target is studied in the paper. The considered power system comprises of N_1 THPs, N_3 WPPs, N_4 SPPPs, and N_5 PSHEPs scheduled over 24 h. The study only considers electricity generation costs for THPs while that for other remaining power plants is neglected. The assumption is derived from the free water in PSHEPs, free wind in WPPs, and free solar radiation in SPPPs. The main task of the sole PSHEP is to effectively use electricity from TPs, WPP and SPPP to store water and cut the fuel cost for the two THPs. The PSHEP’s performance is evaluated by calculating the fuel cost of the THPs. The problem’s objective function is to reduce the generation cost of all THPs by Ref. [45]:

$$Reduce\ GenCost_{tp} = \sum_{t=1}^{N_1} \sum_{iv=1}^{N_2} [ce_{1t} + ce_{2t}TP_{t,iv} + ce_{3t}(TP_{t,iv})^2] \tag{1}$$

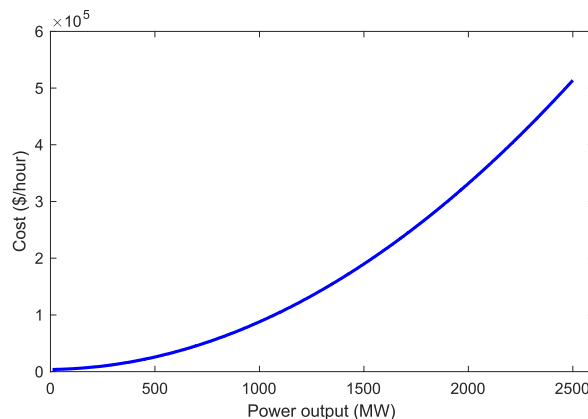


Fig. 2. Power output-fuel cost characteristic of thermal power plants.

2.2. Constraints

Constraints of power systems comprise physical limits for all power plants, hydraulic limits for PSHEPs, and power balance between generation and consumption. All these constraints can be expressed in detail as follows.

2.2.1. Constraints of power balance

Power balance is an essential criterion for the stable state of power systems. When the constraint is satisfied, the frequency can be within a predetermined allowable range. The constraint is that the generation power produced by all power plants must be equal to the total load demand plus the losses on the transmission line as follows [46]:

$$\sum_{t=1}^{N_1} TP_{t,itv} + \sum_{w=1}^{N_3} WP_{w,itv} + \sum_{p=1}^{N_4} PP_{p,itv} + \sum_{m=1}^{N_5} (1 - HPMODE_{m,itv}) \times HP_{m,itv} - \sum_{m=1}^{N_5} (HPMODE_{m,itv}) \times HP_{m,itv}^{pump} - PLOSS_{itv} - PLoad_{itv} = 0; itv = 1, \dots, N_2 \quad (2)$$

In Equation (2), $HPMODE_{m,itv}$ is the operation status of the m th PSHEP at the itv th interval. It has two values, either one or zero, depending on the operation status of the considered m th PSHEP [18]. The operation status has been mathematically presented in Ref. [18], and its mathematical expression can be expanded as follows:

$$HPMODE_{m,itv} = \begin{cases} 1, & \text{if } HP_{m,itv}^{pump} = HP_m^{Up} \text{ and } HP_{m,itv} = 0 \\ 0, & \text{if } HP_{m,itv}^{pump} = 0 \text{ and } HP_{m,itv} \geq 0 \end{cases} \quad (3)$$

Eq. (3) is used to clarify the power balance constraint in Eq. (2); meanwhile, Fig. 3 is plotted to clarify two operation statuses of PSHEPs shown in Eq. (3). In Eq. (3), $HPMODE_{m,itv} = 1$ indicates the PSHEP's pumping mode as shown in Fig. 3a, and $HPMODE_{m,itv} = 0$ indicates the PSHEP's generating mode as shown in Fig. 3b. As performing the pumping mode, $HP_{m,itv}^{pump} = HP_m^{Up}$ and $HP_{m,itv} = 0$ will be substituted into Equation (2). As performing the generating mode, $HP_{m,itv}^{pump} = 0$ and $HP_{m,itv} \geq 0$ will be substituted into Equation (2). So, the PSHEP's operating mode at each hour will decide the result of the power balance constraint.

2.2.2. Constraints of power limits

The generation of power plants must satisfy a predetermined range to ensure economic and technical criteria. A lower generation limit is typically used to assure economic criterion, whereas an upper limit is considered to operate the plants stably and safely. In addition, the PSHEPs are subjected to the pump power limit due to the water storage function. The generation limits of all power plants [8] and the pump power limit of PSHEPs [14] are presented as follows:

$$TP_t^{Low} \leq TP_{t,itv} \leq TP_t^{Up} \quad (4)$$

$$WP_w^{Low} \leq WP_{w,itv} \leq WP_w^{Up} \quad (5)$$

$$PP_p^{Low} \leq PP_{p,itv} \leq PP_p^{Up} \quad (6)$$

$$HP_m^{Low} \leq HP_{m,itv} \leq HP_m^{Up} \quad (7)$$

$$0 \leq HP_{m,itv}^{pump} \leq HP_m^{Up} \quad (8)$$

Among the considered power plants, thermal and hydropower plants can adjust their generation to predetermined values from the

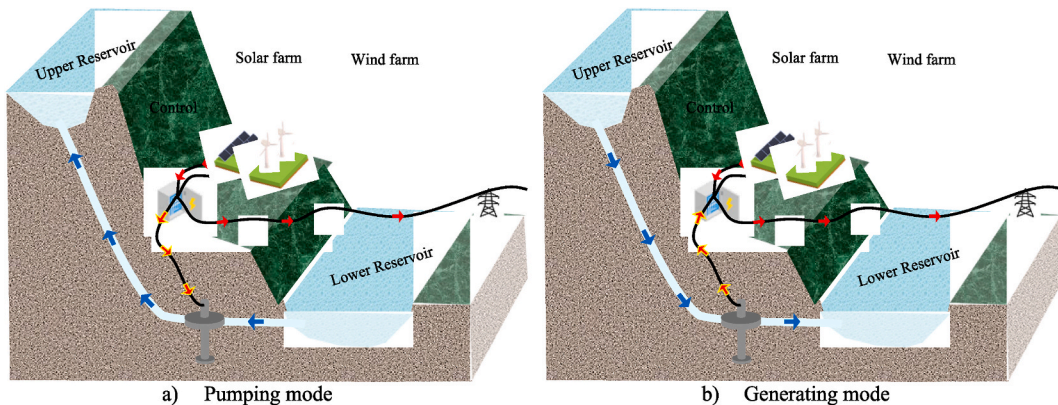


Fig. 3. Operation modes of the PSHEP in a hybrid power system.

optimal schedule, and they can satisfy Eq. (4) and Eq. (7) exactly. The wind and solar power plants can control their generation to satisfy the constraints in Eq. (5) and Eq. (6), but they cannot adjust the generation to equal an expected value. Power generated by the renewable power plants is dependent on the wind speed and solar radiation. The operators can decrease the power output easily, but they cannot increase it. The constraints of PSHEPs are special. The generation limits and pump power limits in Eq. (7) and Eq. (8) are not considered simultaneously. At a given hour, the PSHEP just selects either pumping mode or generating mode. The pump power is either zero or maximum, as presented in Eq. (3).

2.2.3. Hydraulic constraints of PSHEPs

Lower and upper discharge limitations: To satisfy the PSHEPs' generation limits shown in Eq. (7), the water discharge through turbines must be within a predetermined range shown in the following expression [47]:

$$Q_m^{Low} \leq Q_{m,itv} \leq Q_m^{Up} \quad (9)$$

In Equation (9), $Q_{m,itv}$ is the discharge of the m th PSHEP at the itv^{th} interval calculated as follows [14]:

$$Q_{m,itv} = de_{3m}(HP_{m,itv})^2 + de_{2m}HP_{m,itv} + de_{1m} \quad (10)$$

Where de_{1m} , de_{2m} and de_{3m} are known coefficients of the considered m th PSHEP. As the discharge is obtained by using optimization, Eq. (10) is employed to calculate the generation $HP_{m,itv}$ for the m th PSHEP at the itv^{th} interval.

Lower and upper limitations of volume: The water head of the PSHEPs' upper reservoir is always supervised to guarantee that it is within the allowable range. The water head limitation is converted into the reservoir's volume as shown in the following inequality [48]:

$$V_m^{Low} \leq V_{m,itv} \leq V_m^{Up} \quad (11)$$

Water balance constraints: At each interval, the water in the reservoir must satisfy the equality constraint below [46]:

$$V_{m,itv-1} + IW_{m,itv} - V_{m,itv} - (1 - HPMODE_{m,itv}) \cdot Q_{m,itv} + HPMODE_{m,itv} \cdot Q_{m,itv}^{pump} = 0 \quad (12)$$

In Equation (12), $Q_{m,itv}^{pump}$ is the pumping flow of the m th PSHEP at the itv^{th} interval and it is the same for different intervals with pumping mode. The parameter is calculated by using the upper discharge and efficiency of the m th PSHEP as follows [14]:

$$Q_{m,itv}^{pump} = Ef_m \cdot Q_m^{Up} \quad (13)$$

In Equation (13), Ef_m is the pumping efficiency of the m th PSHEP, and it is selected to be 0.75 [14]. For example, it used 100 MWh to run a pump over 1 h to store water. However, it reaches 75 MWh for 1 h if it discharges the stored water to produce electricity. In other words, when PSHEP discharges 100 m³ per second, it can produce a power of 100 MW; however, it just stores 75 m³ per second when it runs the pumps with 100 MW. It means that PSHEP loses 25 % of its electricity or 25 % of its water.

Initial and end reservoir volumes constraints: Initial reservoir volume is the available water in the reservoir at the beginning of one operating day, and end reservoir volume is the remaining water after one operating day. The study considers the same value for the two factors as shown in the following equation [49]:

$$V_{m,N_1} = V_{m,0} \quad (14)$$

Where.

$V_{m,0}$ = Initial volume of the reservoir in the m th PSHEP

V_{m,N_1} = Volume of the reservoir in the m th PSHEP at the end of the last interval

In the paper, the two parameters are required to be the same in two scenarios. In Scenario 1, the PSHEP only produces electricity and does not run pumps to store water. In Scenario 2, the PSHEP can run the pump to store water and produce electricity. So, PSHEP is working as a conventional hydropower plant (CHEP) in Scenario 1. The constraint (14) assures that the two scenarios are fair for the two power plants: CHEP and PSHEP. CHEP only uses inflows of water to produce electricity in Scenario 1. PSHEP can use inflows and stored water to produce electricity in Scenario 2.

2.3. Generation power of wind and solar photovoltaic power plants

The power produced by wind and photovoltaic power plants depends on wind speed and solar radiation. In the study, wind speed and solar radiation are supposed to be given and are certain over one scheduled day. From those data, the power of wind and solar photovoltaic power plants can be determined by Refs. [50,51]:

$$WP_{w,itv} = \begin{cases} 0, & (Ve_{w,itv} < Ve_w^{Low} \text{ or } Ve_{w,itv} > Ve_w^{Up}) \\ WP_w^{Rate} \times \frac{(Ve_{w,itv} - Ve_w^{Low})}{(Ve_w^{Rate} - Ve_w^{Low})}, & (Ve_w^{Low} \leq Ve_{w,itv} \leq Ve_w^{Rate}) \\ WP_w^{Rate} & (Ve_w^{Rate} \leq Ve_{w,itv} \leq Ve_w^{Up}) \end{cases} \quad (15)$$

$$PP_{p,itv} = \begin{cases} PP_p^{Rate} \times \frac{(SR_{p,itv})^2}{(CIP_w \cdot SR_p)}, & (0 < SR_{p,itv} < SR_p) \\ PP_p^{Rate} \times \frac{SR_{p,itv}}{CIP_w}, & (SR_{p,itv} \geq SR_p) \end{cases} \quad (16)$$

Where, Ve_w^{Low} and Ve_w^{Up} are the lowest and highest wind speeds that wind turbines in the w th WP can produce electricity. WP_w^{Rate} is the rated power of the w th wind power plant. Ve_w^{Rate} is the rated wind velocity in the w th wind power plant associated with the rated power WP_w^{Rate} . PP_p^{Rate} is the rated power of the p th photovoltaic power plant. It is noted that the rated powers of the w th WPP and the p th SPPP (i.e., WP_w^{Rate} and PP_p^{Rate}) are also upper generation limits, WP_w^{Up} and PP_p^{Up} shown in Equations (5) and (6), respectively.

3. 3. jellyfish search algorithm (JSA)

Jellyfish search algorithm (JSA) is a highly effective meta-heuristic algorithm developed in 2020 by J. S. Chou and D.N. Truong [30]. The main idea to form the algorithm is derived from two methods of jellyfish movements in the ocean, including ocean current and swarm current. Also, from the two movements, JSA also updates promising solutions with two methods, and JSA can perform better than many algorithms thanks to the new features. The basic structure of JSA is comprised of three main steps as follows.

3.1. The population initialization

For each optimization, decision variables, known as the sole parameters of an optimal solution, are first chosen before implementing optimization tools to find a final optimal solution. The decision variables have an allowable range between upper bound UpB and lower bound LoB , and each solution in the population is initially produced based on the bounds as follows:

$$S_i = LoB + \omega_i \times (UpB - LoB) \text{ with } i = 1, \dots, N_{PZ} \quad (17)$$

3.2. New solution update mechanisms

As mentioned, JSA has two update mechanisms according to two movement methods. For all solutions, the two methods are used simultaneously at the same iteration, but one out of the two methods is employed at each computation iteration. So, JSA needs a selection condition based on comparing the selection factor (SF) and a balance factor (BF). SF is determined by using the current iteration (IT_{cur}) and the maximum iteration number (IT_{max}), while BF is selected as 0.5. Equation (18) is applied to calculate SF .

$$SF = \left(1 - \frac{IT_{cur}}{IT_{max}}\right) \times (2 \times rdn - 1) \quad (18)$$

If SF is greater or equal to 0.5, JSA will update its new solutions by using the mechanism based on the ocean current. Otherwise, the new solutions will be updated by using another mechanism based on the movement of the jellyfish swarm. The mechanism based on the ocean current can be known as the exploration phase, while the mechanism based on the movement of the jellyfish swarm is the exploitation phase. These two mechanisms are described as follows.

3.2.1. The exploration phase

The exploration phase will be applied to update new solutions if the selection factor SF is equal to or higher than the balance factor BF . The exploration phase in JSA has the same feature as that in Cuckoo search algorithm (CSA) since the best solution is used to produce an increased interval. However, JSA is simpler than CSA because it does not use Levy flight distribution. In fact, the simplification of JSA can be seen as shown in the following equation:

$$S_i^{new} = S_i + rdn \times (S_{Best} - 3 \times rdn \cdot S_{mean}) \quad (19)$$

Where, S_i^{new} is the new location of the i th jellyfish; S_{Best} is the best current position in the whole swarm; and S_{mean} is the mean position in the whole swarm obtained by:

$$S_{mean} = \frac{\sum_{i=1}^{N_{PZ}} S_i}{N_{PZ}} \quad (20)$$

3.2.2. The exploitation phase

The exploitation phase is critical to exploit search spaces carefully and effectively. Many metaheuristic algorithms can be successful by using the exploitation phase, such as variants of CSA [52] and Differential Evolution [53]. JSA also highly values the function of the exploitation phase, and it applies two models for the mechanism as follows:

$$S_i^{new} = \begin{cases} S_i + Ds, & \text{if } rdn \leq (1 - NF) \\ S_i + 0.1 \times \omega_i \times (UpB - LoB), & \text{otherwise} \end{cases} \quad (21)$$

In Equation (21), Ds is the increased interval between the current location of the i th and $(i+1)^{th}$ jellyfish. The step can be calculated by:

$$Ds = |S_{i+1} - S_i| \quad (22)$$

Where S_{i+1} is the current location of the $(i+1)^{th}$ jellyfish in the swarm.

3.3. Selection technique

After all jellyfish update their new locations, the evaluation and comparison will occur based on the fitness function calculation. This action aims to select the high-quality solution for the next iteration and abandon the poor ones to discard the search in the zones. The mathematical expression of the evaluation is presented as follows:

$$S_i = \begin{cases} S_i^{new} & \text{if } FS_i^{new} < FS_i \\ S_i & \text{else} \end{cases} \quad \text{with } i = 1, \dots, N_{Pz} \quad (23)$$

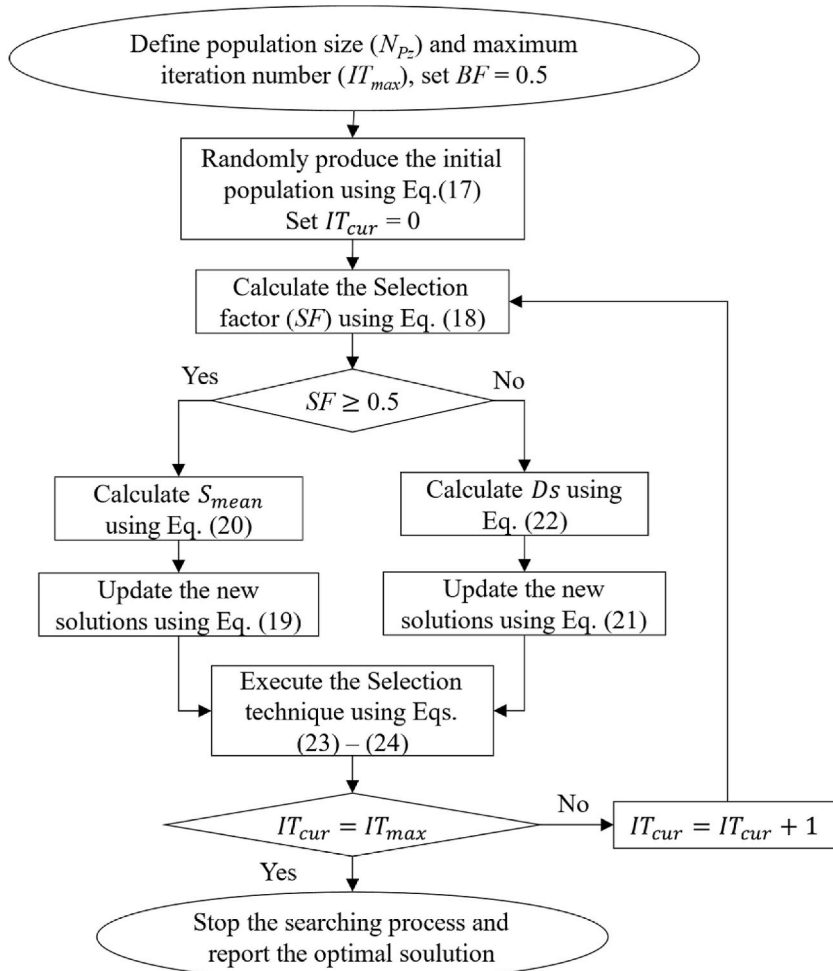


Fig. 4. Computation steps of JSA for the solved problem.

$$FS_i = \begin{cases} FS_i^{new} & \text{if } FS_i^{new} < FS_i \\ FS_i & \text{else} \end{cases} \text{ with } i = 1, \dots, N_{PZ} \tag{24}$$

Finally, the best solution in the current population is determined by finding the lowest fitness value in the swarm. If the current computation iteration is equal to the maximum iteration number, the best solution will be saved as one effective solution candidate. Otherwise, the following iteration will be implemented until the maximum iteration is reached. Fig. 4 presents the application of JSA for a typical optimization problem.

4. Numerical results

In this Section, two different power systems with the energy storage ability from the sole PSHEP are optimally scheduled over one day within 24 h. Power losses are neglected in the two systems. The first system is comprised of two THPs and one PSHEP. The second system is modified from the first system by combining the first system with two other renewable power plants: one SPPP and one WPP. The parameters of the two THPs are taken from Ref. [46] and shown in Table A1. The data of the PSHEP are taken from Ref. [14] and shown in Table A2. The flows and load demand are modified from Ref. [46] and reported in Table A3. The second system’s solar radiations and wind speeds are taken from Refs. [51,54]. Substituting the data into Equations (15) and (16), the power generations are obtained and reported in Table A4 in Appendix. For each test system, two study cases are implemented as follows.

Case 1. The PSHEP only produces electricity as a conventional hydropower plant (CHEP).

Case 2. The PSHEP can run the pump to store water and produce electricity.

This study has applied six recently published algorithms, including TSA, ASBO, JSA, NGA, AHA, and WSOA, to verify the vast potential of PSHEPs and find the most suitable algorithm for the complex optimization in power systems. In each computation iteration, ASBO, WSOA, and NGA perform two update processes to reach new solutions, but TSA, AHA, and JSA only perform one update process to reach new solutions. So, the same iteration number of 30,000 is set for all algorithms but different population sizes. The population size is 50 for ASBO, WSOA, and NGA but 100 for TSA, AHA, and JSA. As a result, all applied algorithms have the same newly updated solution number: $(50 \times 2 \times 30,000 = 3,000,000)$ for ASBO, WSOA, and NGA and $(100 \times 1 \times 30,000 = 3,000,000)$ for TSA, AHA, and JSA. The number of newly updated solutions is also the number of fitness evaluations, so all algorithms are fairly compared. On the other hand, the settings can lead to an approximately equal average computation time for all algorithms. For each study case, fifty runs are executed for each algorithm. The algorithms employed are implemented on MATLAB software using a computer with a processor of 2.20 GHz and a RAM of 4 GB.

4.1. Comparisons of result for the first system

In this section, the first system with two THPs and one PSHEP is employed to test the performance of six applied algorithms. The configuration of the system is given in Fig. 5. Each algorithm is executed for fifty trial runs for each study case, and the fifty generation cost values from fifty obtained solutions are reported in Fig. 6. JSA has the best search stability once all fifty generation cost values in

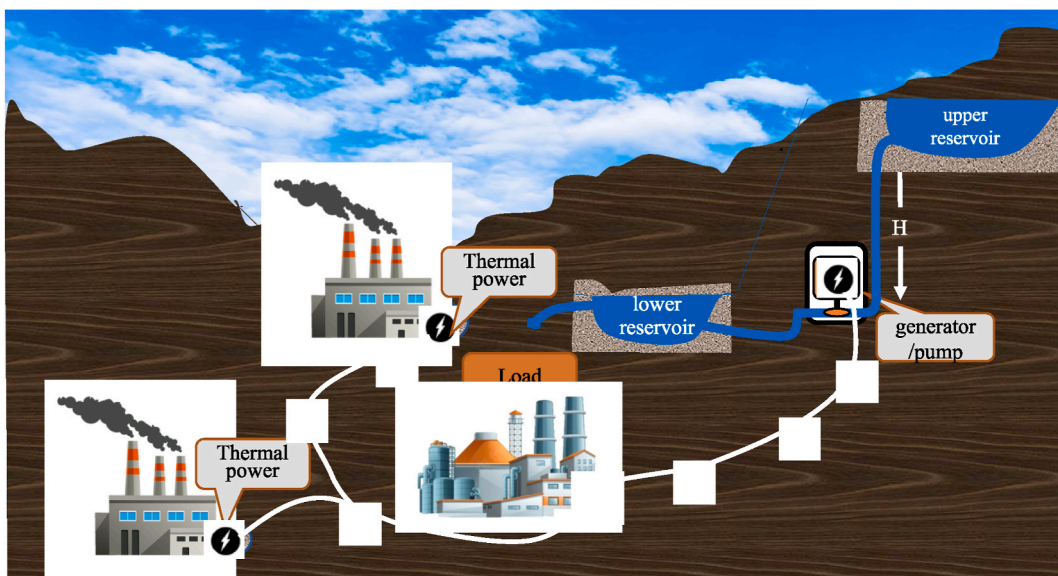


Fig. 5. The first system.

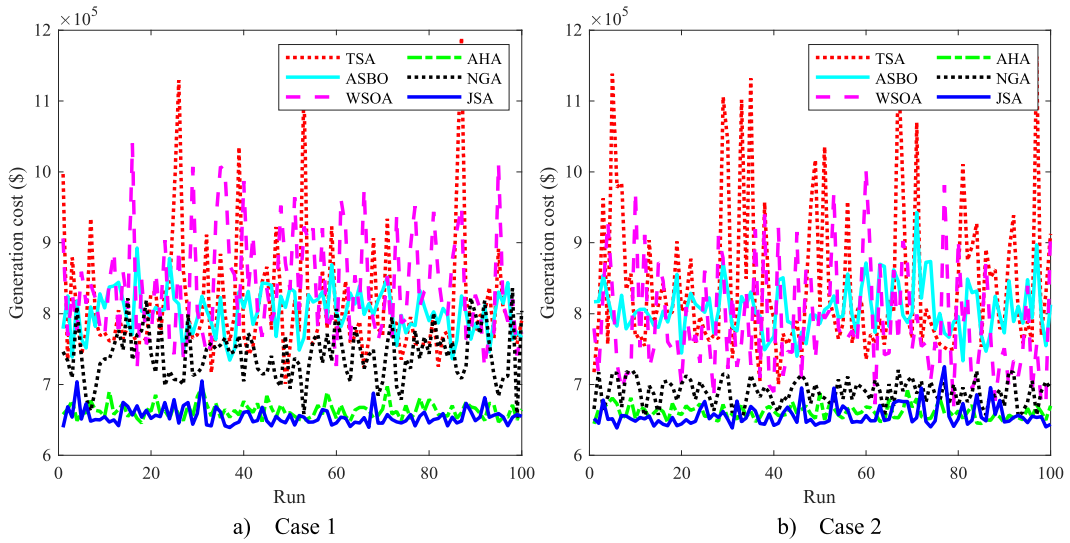


Fig. 6. Fuel cost obtained by six applied methods for fifty runs for the first system.

the blue are smaller than those of others.

Fig. 7 depicts the savings compared between the costs of JSA and those of others, which are described in percentages. In Case 1, the best cost of JSA is smaller than that of TSA by 8.78 %, ASBO by 12.92 %, WSOA by 11.38 %, AHA by 0.99 %, and NGA by 3.8 %. In Case 2, JSA can reduce the minimum cost from 0.91 % to 12.94 %, the mean cost from 0.67 % to 22.03 %, and the maximum cost from 23.08 % to 37.62 %. Only AHA can reach smaller maximum costs than JSA for the two cases. Fig. 8 plots the best run of the fitness function at each computation iteration where JSA can find better solutions than others at the 1,300th iteration for Case 1 and at the 1,900th iteration for Case 2. Thus, JSA is likely to converge to the optimal solutions faster than others. As a result, JSA is the best method for this optimization problem regarding fair comparison criteria, such as low fuel cost, stable ability, and fast convergence search.

4.2. Comparisons of result for the second system

The second system shown in Fig. 9 is employed to run the six applied algorithms in the section. The generation costs are collected and reported in detail in Fig. 10; meanwhile, Fig. 11 presents the saving cost (in %) of JSA as compared to others. JSA can reach lower generation costs than others by from 0.58 % to 13.34 % for the minimum cost in Case 1 and from 1.07 % to 11.79 % for the minimum cost in Case 2. For other costs, JSA also reaches high saving costs compared to others, excluding the comparison with AHA for

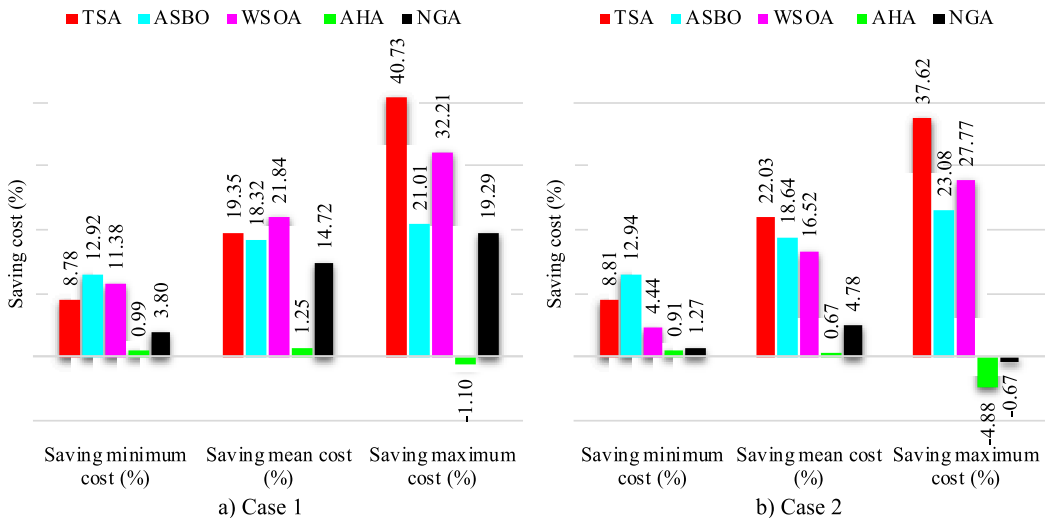


Fig. 7. Saving cost of JSA as compared to others for the first system.

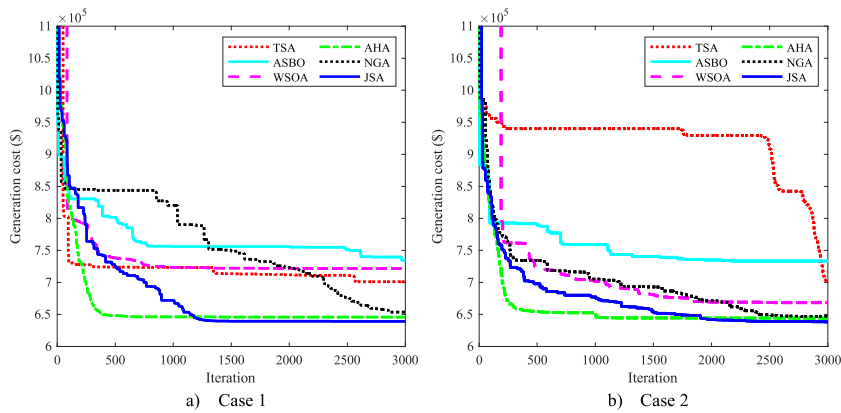


Fig. 8. Fitness function at each computation iteration from the best run obtained by six applied methods for the first system.

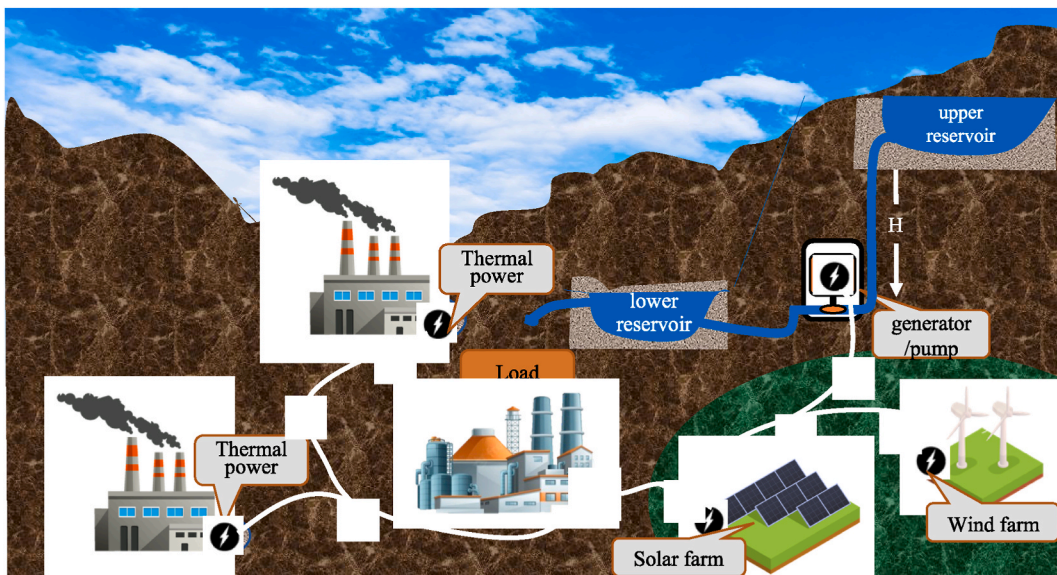


Fig. 9. The second system.

maximum cost in Case 2. Fig. 12 describes the convergence characteristics of implementation iterations of all applied algorithms. JSA is much faster than almost all compared algorithms, excluding AHA, which is faster than local optimums but cannot exist in the zones to reach better solutions than JSA. Here, we need to discuss the disadvantages and advantages of JSA as we see the convergence characteristics. From iterations 1 to 2,000, we can understand that if the iteration number is just set to 2,000, JSA is still more effective than TSA, ASBO, WSOA, and NGA for both Case 1 and Case 2. However, at the 2000th iteration, the generation costs of JSA are still greater than those of AHA. If the search is terminated at the 2,000th iteration, JSA is worse than AHA. From iteration 2000 to the last iteration, JSA has a special search ability not to fall into local optimums as AHA. Finally, JSA is the best performance algorithm to reach the best stability and to find the highest quality solutions.

4.3. Contribution of PSHEP to fuel cost reduction

In the section, the contribution of PSHEP to the fuel cost reduction is clarified. The total generation cost of the power systems with CHEP (Case 1) and PSHEP (Case 2) is obtained. The significant contributions of PSHEP are explicitly analyzed by comparing the generation costs of two study cases at each test power system implemented by six algorithms. Saving cost or the generation cost reduction of Case 2 compared to Case 1 in dollars and percentages is obtained by using the following equations:

$$\text{Saving cost (\$)} = \text{Case 1's } GenCost_{tp} - \text{Case 2's } GenCost_{tp} \tag{25}$$

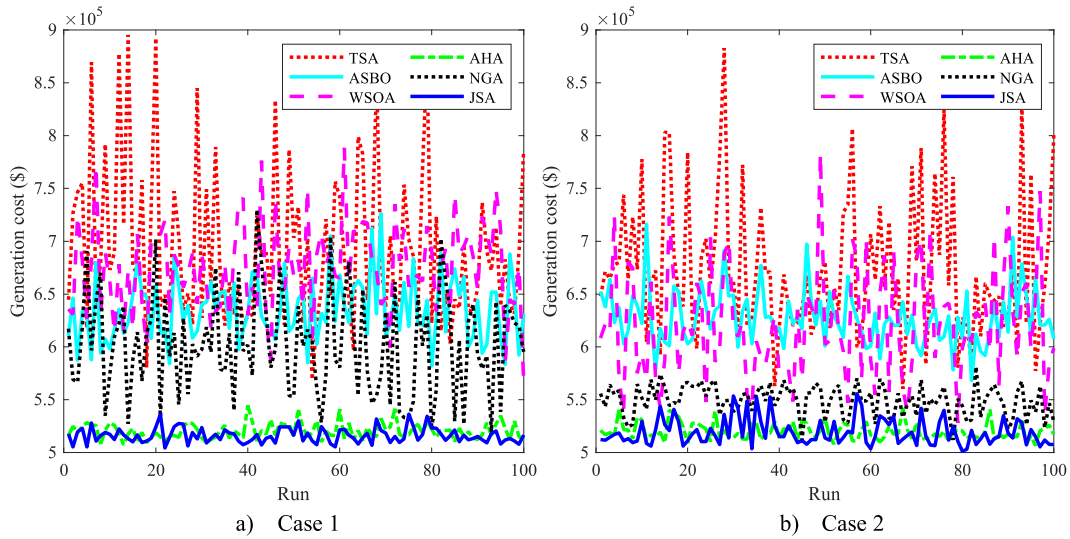


Fig. 10. Fuel cost obtained by six applied methods for fifty runs for the second system.

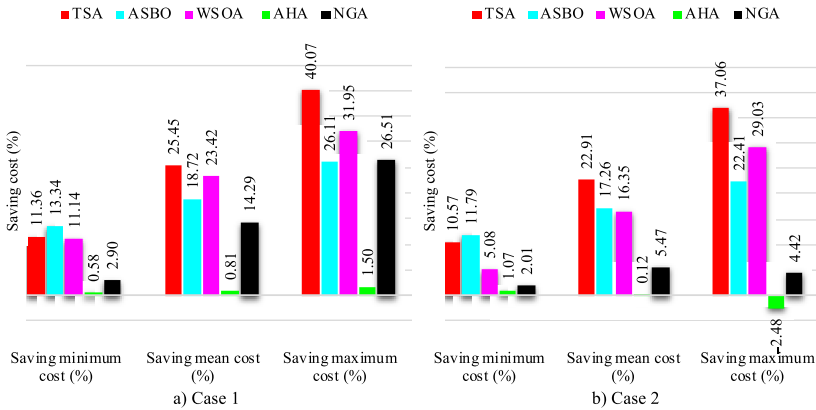


Fig. 11. Saving cost of JSA as compared to others for the second system.

$$Saving\ cost\ (\%) = \frac{Saving\ cost\ (\$)}{Case\ 1's\ GenCost_{ip}} \cdot 100 \tag{26}$$

In Equation (25), $GenCost_{ip}$ in \$ is the total generation cost of all thermal power plants obtained by using Equation (1). The cost of Case 1 and Case 2, and saving cost are presented in detail in Table 1 for System 1 and Table 2 for System 2. In addition, the saving cost values in \$ and % are summarized in Fig. 13. The cost reduction proves PSHEP’s outstanding performance over CHEP. All six applied algorithms achieved significant cost reduction. TSA, ASBO, WSOA, AHA, NGA, and JSA could reach the saving cost of \$748.9, \$902.5, \$53,359.7, \$1451.5, \$17,908.8, and \$886.6 (corresponding to 0.11, 0.12, 7.4, 0.22, 2.69, and 0.14 % respectively) for the first system, and \$8494.8, \$13,744.3, \$39,472.8, \$640.2, \$7878.5, and \$3091.4 (corresponding to 1.49, 2.36, 6.95, 0.13, 1.52, and 0.61 % respectively) for the second system. In other words, PSHEP is more effective than CHEP in supporting the two power systems to reach smaller electricity generation costs.

Many previous studies stated the effectiveness of PSHEPs by showing cost reduction values or obtained benefit values; however, these studies only applied one or a few popular algorithms. The limit could not ensure that the obtained solutions reported in previous studies were high quality, and the PSHEPs might have more potential than reported results. In the study, the implementation of JSA and the five other algorithms aimed to find the most optimal solutions for the two test systems, and the most optimal obtained solutions can reflect the actual effectiveness of pumped storage hydropower plants in the hybrid power systems. The significant solutions are analyzed to clarify the contributions of the study.

Fig. 14 presents the generation of the PSHEP at each hour and accumulative energy from the first hour to each considered hour for the two systems. By observing orange bars with up and down directions, we can calculate that there are 5 h with the pumping mode and 9 h with the generation mode on the first system, and there are 3 h with the pumping mode and 8 h with the generation mode on

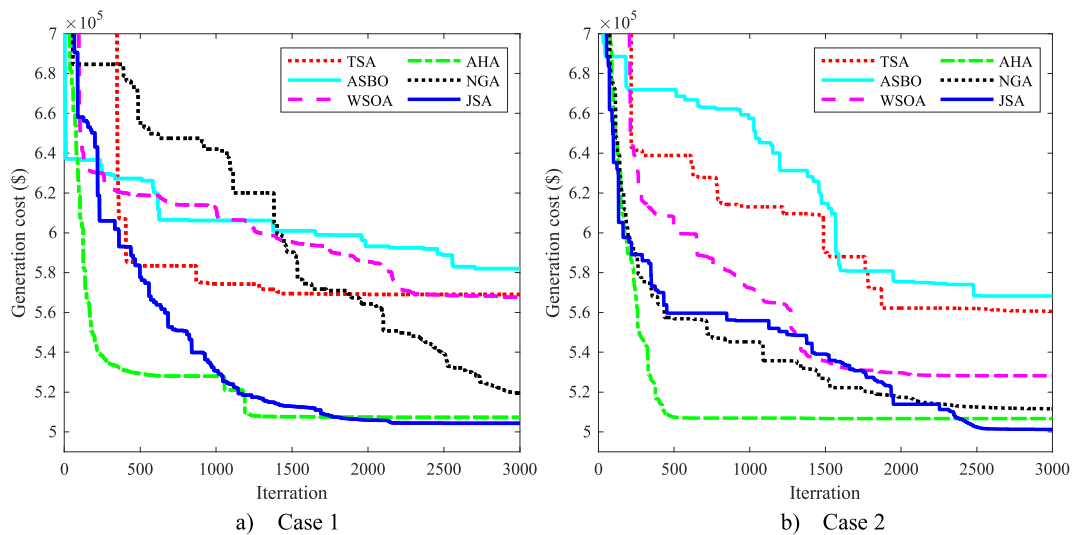


Fig. 12. Fitness function at each computation iteration for the best run obtained by six applied methods for the second system.

Table 1

Cost comparison between Case 1 and Case 2 obtained by each algorithm for System 1.

Method	TSA	ASBO	WSOA	AHA	NGA	JSA
Cost of Case 1 (\$)	700968.5	734317.3	721540.0	645837.5	664672.3	639417.5
Cost of Case 2 (\$)	700219.6	733414.8	668180.3	644386.0	646763.5	638530.9
Saving cost (\$)	748.9	902.5	53,359.7	1451.5	17,908.8	886.6
Saving cost (%)	0.11	0.12	7.40	0.22	2.69	0.14

Table 2

Cost comparison between Case 1 and Case 2 obtained by each algorithm for System 2.

Method	TSA	ASBO	WSOA	AHA	NGA	JSA
Cost of Case 1 (\$)	568976.2	582011.0	567585.2	507301.9	519426.1	504352.6
Cost of Case 2 (\$)	560481.4	568266.8	528112.5	506661.7	511547.6	501261.2
Saving cost (\$)	8494.8	13,744.3	39,472.8	640.2	7878.5	3091.4
Saving cost (%)	1.49	2.36	6.95	0.13	1.52	0.61

the second system. Using the height of the orange bars, we find PSHEP has produced 2450 MWh but consumed 1500 MWh for pumping water on the first system. Similarly, it has produced 1950 MWh but consumed 900 MWh for pumping water on the second system. So, the total energy is 950 MWh on the first system and 1050 MWh on the second system. From the figures, we can see the results by seeing the last points of the blue and orange dash curves with the numbers 1350 and 950 MWh for Case 1 and Case 2 of the first system and the numbers 1350 and 1050 MWh for Case 1 and Case 2 of the second system. There is a strange issue here for the two systems because Case 2 reaches smaller energy than Case 1. It means the PSHEP is not effective in reaching higher energy if it runs pumps to store water. This consequence is due to the pump efficiency shown in Equation (13), which is 0.75, as reported in Table A2 in the Appendix. However, the considerable contribution of the PSHEP is not for reaching high energy but for reducing the total electric generation cost for thermal power plants. In fact, in Fig. 13, we can see the evidence clearly. Methods could reach smaller costs for Case 2 than Case 1 by, from 0.11 % to 7.4 % for the first system and from 0.13 % to 6.95 % for the second system. For JSA, the saving cost of JSA shown in Fig. 13 is \$886.6 on System 1 and \$3091.4 on System 2, thanks to the pumping function of PSHEPs.

Fig. 15 is plotted to clarify the results from Fig. 14. In Fig. 15, we can see the difference between Case 1 and Case 2 of each system. Case 2 has four parameters: volume, inflows, discharge, and stored water. The stored water results from running the pump, whereas Case 1 only has the three first parameters except for stored water. The red area expresses the inflows. The yellow and dark blue areas show discharge and storage water. Blue areas are the reservoir volume at the end of each hour. Discharges are shown using negative values because they decrease the reservoir's volume. The inflows and stored water values are positive because they cause the reservoir's volume to go up. In Fig. 15, the smallest discharges are 695.6, 553.8, 466.0, and 534.2 acre-ft, but the greatest discharges are 800 or smaller than 800 acre-ft. In Fig. 15b and d, the stored water has reached only two values, 0 or 600 acre-ft. The greatest reservoir volume of Case 2 in the two systems is 9850 acre-ft at hour 7, whereas the smallest reservoir volume is 4400 and 5600 acre-ft at the same hour 17 for both systems. Case 1 has the greatest reservoir volume of 9650 acre-ft at hour 11 for System 1 and 9550 acre-ft at hour

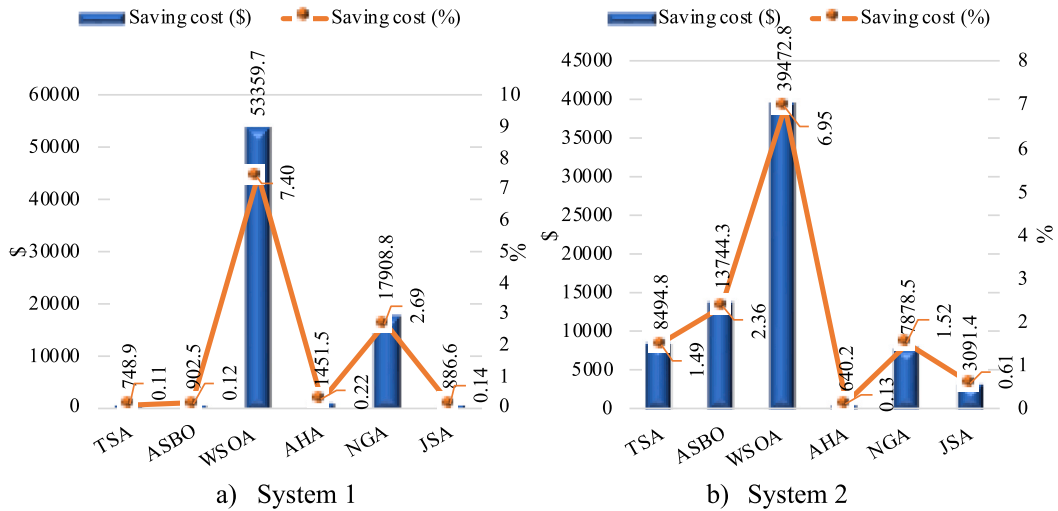


Fig. 13. Saving cost of Case 2 as compared to Case 1 obtained by six applied algorithms.

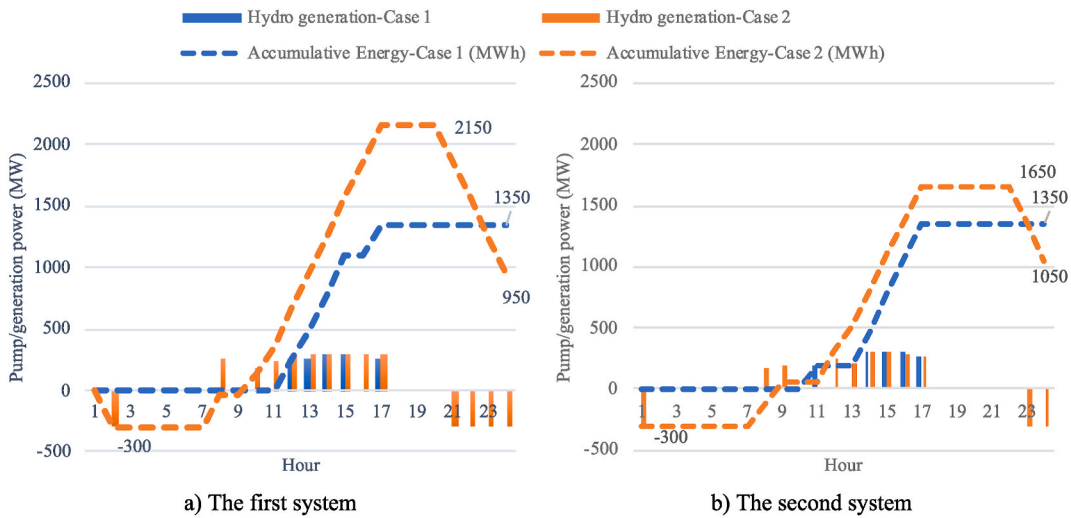


Fig. 14. Hydro generation and accumulative energy for Case 1 and Case 2 of the two systems.

10 for System 2, and the smallest reservoir volume of 6800 acre-ft at hour 17 in the two systems. The initial and end reservoir volumes in Fig. 15 are the same and equal to 8000 acre-ft. As shown in Table A2, the minimum and maximum reservoir volume limits are 3000 and 15,000 acre-ft, respectively, and the maximum discharge is 800 acre-ft. On the other hand, the initial and end reservoir volumes are the same and equal to 8000 acre-ft. So, the hydraulic constraints shown in Section 2.2.3 were proved to be exactly satisfied.

Figs. 16 and 17 are plotted to clarify the cause that Case 2 always has a smaller generation cost than Case 1 for the two systems. In the first system, we stack up the generation of power plants. In the first system, the generation of PSHEP is at the bottom, while that of the second THP is at the top. So, the top of the second THP is equal to the load demand. In the second system, the generation of SPPP is stacked with the second THP, and the generation of the WPP is at the top. At hours 9–17 with high load demand, the generation of PSHEP in Case 2 accounts for a higher area than that in Case 1 for both systems. During other hours with load demand, PSHEP used the power of the second THP to pump water. Hence, Case 2 can reduce the generation of THPs at high load demand, and it is more successful in cutting generation costs.

5. Conclusions

The paper applied six metaheuristic algorithms, including TSA, ASBO, JSA, NGA, AHA, and WSOA, for a complicated optimization problem with the integration of pumped storage hydroelectric plants into thermal power plants, wind power plants, and solar photovoltaic power plants. When applying these algorithms, their first main task was to determine hours with generation mode/pump

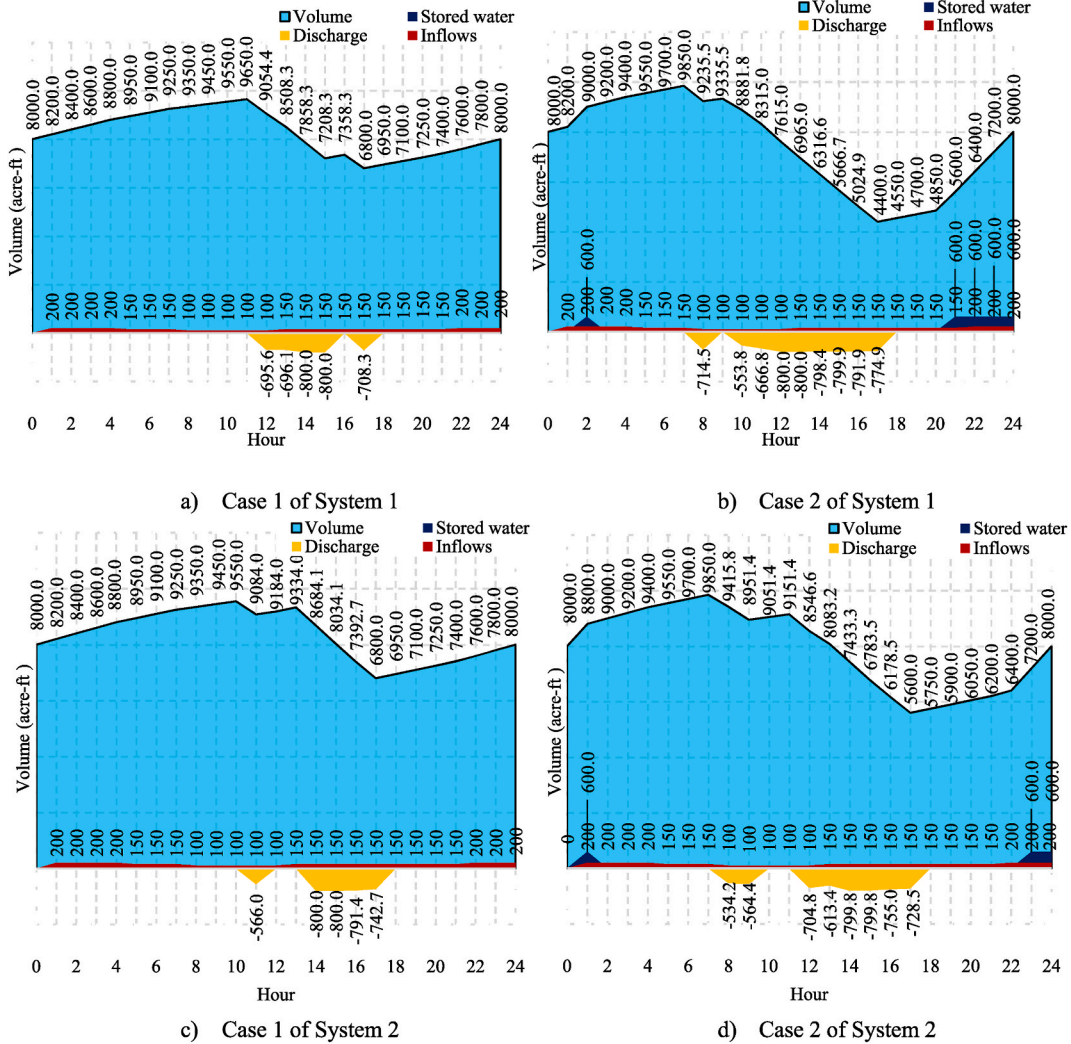


Fig. 15. Reservoir of PSHEP in two study cases of each system.

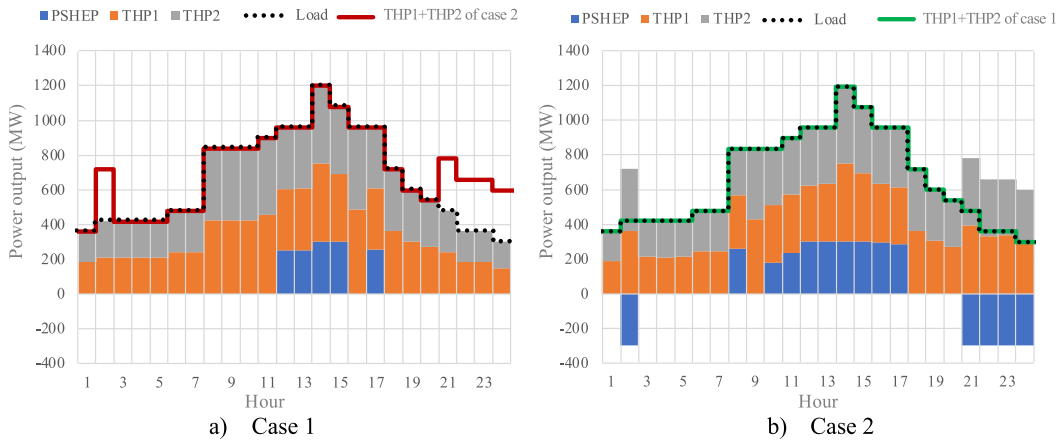


Fig. 16. Generation of power plants in the first system.

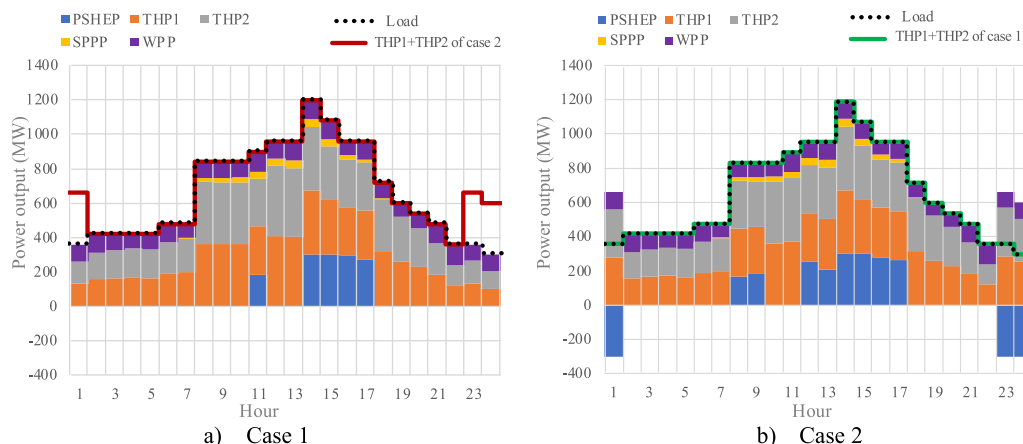


Fig. 17. Generation of power plants in the second system.

modes for the hydroelectric plants. The second main task was to determine the power allocation between PSHPs at hours in generation mode and thermal power plants. The objective of the problem was to reach the minimum generation cost from all thermal power plants, and this cost value was used to find the most effective algorithm and the best optimal generation solutions for test systems. The first test system was comprised of two THPs and one PSHEP, while the second system was the combination of the first system, one wind power plant, and one solar power plant. The study implemented two cases of PSHEP's operation: **Case 1**) PSHEP operated in only generation mode and without pump mode as a conventional hydroelectric plant, and **Case 2**) PSHEP could implement either generation or pump mode. The results from the two cases for two test systems were compared and analyzed, and the whole simulation results of the study can be summarized as follows.

1. The six applied algorithms could successfully find optimal electricity generation solutions for all power plants, as well as optimal water discharge and storage solutions for PSHEP. The power systems' power balance constraint and generation limits and the PSHEP's hydraulic constraints were exactly satisfied. The total generation of all power plants was equal to load demand at hours with pumping mode, and the total generation of wind, solar, and thermal power plants was equal to the sum of load demand and pump power. The initial and end volumes were the same as required; the sum of the inflows and storage water was equal to the discharge.
2. Because of the effectiveness of the PSHEP, all algorithms have reached smaller generation costs for the power systems with PSHEP than for those with CHEP. The cost reduction obtained by TSA, ASBO, WSOA, AHA, NGA, and JSA was 0.11 %, 0.12 %, 7.4 %, 0.22 %, 2.69 % and 0.14 % respectively for the first system, and 1.49 %, 2.36 %, 6.95 %, 0.13 %, 1.52 % and 0.61 % respectively for the second system. Namely, the highest cost reduction was \$53,359.7 for the first system and \$39,472.8 for the second system.
3. JSA was the most suitable algorithm for the two employed systems. JSA could reach lower generation costs than others, from about 1 % to 13 % for the two power systems. JSA has reached a much smaller standard deviation than others for fifty trial runs.

The mentioned results can show the study's main contributions; however, the study has only investigated two aspects: finding the most suitable algorithm for the two applied systems and the high effectiveness of PSHEP in integrated power systems. However, the study has not considered and proposed more effective solutions to real national power systems shown in literature, such as Portugal [17], Iran [18], China [19,20], Spain [21], Turkey [22], and Saudi Arabia [23] due to the lack of input data. In addition, transmission power networks and the spot market have not been concerned. So, future studies will expand the scope and limitations of proving the performance of PSHEP in real power systems. JSA and other new algorithms will be applied to reach reliable and high-quality solutions for future work.

Data availability

Data of the two systems are included in Appendix of the article.

CRediT authorship contribution statement

Phu Trieu Ha: Writing – original draft, Software, Data curation, Conceptualization. **Bach Hoang Dinh:** Writing – review & editing, Methodology, Investigation, Funding acquisition. **Tan Minh Phan:** Software, Resources, Project administration. **Thang Trung Nguyen:** Writing – review & editing, Visualization, Validation.

Declaration of competing interest

The authors declare that they have no known competing financial interests or personal relationships that could have appeared to influence the work reported in this paper

Acknowledgment

This research is funded by Ton Duc Thang University under Grant number FOSTECT.2022.14.

APPENDIX

Table A1
Parameters of two THPs in two systems

t	TP_t^{Low} (MW)	TP_t^{Up} (MW)	ce_{1t}	ce_{2t}	ce_{3t}
1	10	2500	3877.5	3.9795	0.0800
2	10	2500	3900	3.9000	0.0810

Table A2
Parameters of the sole PSHEP in two systems

m	Ef_m	de_{3m}	de_{2m}	de_{1m}	$V_m^{Low}; V_m^{Up}$ (acre-ft)	$HP_m^{Low}; HP_m^{Up}$ (MW)	$V_{m,0}; V_{m,N1}$ (acre-ft)
1	0.75	0	2	200	3000; 15,000	0; 300	8000

Table A3
Inflows and loads for two test systems

itv	$IW_{1,itv}$ (acre-ft)	$PLoad_{itv}$ (MW)	Itv	$IW_{1,itv}$ (acre-ft)	$PLoad_{itv}$ (MW)	itv	$IW_{1,itv}$ (acre-ft)	$PLoad_{itv}$ (MW)
1	200	360	9	100	840	17	150	960
2	200	420	10	100	840	18	150	720
3	200	420	11	100	900	19	150	600
4	200	420	12	100	960	20	150	540
5	150	420	13	150	960	21	150	480
6	150	480	14	150	1200	22	200	360
7	150	480	15	150	1080	23	200	360
8	100	840	16	150	960	24	200	300

Table A4
Generation of SPPP and WPP for the second system

itv	$PP_{1,itv}$ (MW)	$WP_{1,itv}$ (MW)	itv	$PP_{1,itv}$ (MW)	$WP_{1,itv}$ (MW)
1	0	99	13	45.695	111.6
2	0	108	14	47.84	109.2
3	0	93	15	38.09	111
4	0	82.8	16	27.625	81
5	0	90	17	18.915	105
6	0	106.8	18	3.20493333	91.2
7	5.3391	81.6	19	0	78
8	20.215	93	20	0	82.8
9	24.375	94.8	21	0	114
10	32.695	86.4	22	0	120
11	40.105	120	23	0	92.4
12	44.59	99	24	0	96

References

[1] J. Gao, Y. Zheng, J. Li, X. Zhu, K. Kan, Optimal model for complementary operation of a photovoltaic-wind-pumped storage system, *Math. Probl Eng.* 2018 (2018) 1–9, <https://doi.org/10.1155/2018/5346253>.
 [2] E. Barbaros, I. Aydin, K. Celebioglu, Feasibility of pumped storage hydropower with existing pricing policy in Turkey, *Renew. Sustain. Energy Rev.* 136 (2021) 110449, <https://doi.org/10.1016/j.rser.2020.110449>.
 [3] V. Pandey, A. Sircar, K. Yadav, N. Bist, Pumped hydro storage for intermittent renewable energy: present status and future potential in India, *MRS Energy & Sustainability* 10 (2023) 189–206, <https://doi.org/10.1557/s43581-023-00064-0>.

- [4] M. Kharrich, S. Kamel, M. Abdeen, O.H. Mohammed, M. Akherraz, T. Khurshaid, S.-B. Rhee, Developed Approach based on equilibrium optimizer for optimal design of hybrid PV/Wind/Diesel/Battery microgrid in Dakhla, Morocco, *IEEE Access* 9 (2021) 13655–13670, <https://doi.org/10.1109/ACCESS.2021.3051573>.
- [5] M. Kharrich, L. Abualigah, S. Kamel, H. AbdEl-Sattar, M. Tostado-Véliz, An improved arithmetic optimization algorithm for design of a microgrid with energy storage system: case study of El Kharga Oasis, Egypt, *J. Energy Storage* 51 (2022) 104343, <https://doi.org/10.1016/j.est.2022.104343>.
- [6] M. Kharrich, A. Selim, S. Kamel, J. Kim, An effective design of hybrid renewable energy system using an improved Archimedes Optimization Algorithm: a case study of Farafra, Egypt, *Energy Convers. Manag.* 283 (2023) 116907, <https://doi.org/10.1016/j.enconman.2023.116907>.
- [7] X. Wu, Y. Wu, Q. Ying, Research on dynamic programming game model for hydropower stations, *Math. Probl. Eng.* 2022 (2022) 1–11, <https://doi.org/10.1155/2022/1458388>.
- [8] L.H. Pham, B.H. Dinh, T.T. Nguyen, Optimal power flow for an integrated wind-solar-hydro-thermal power system considering uncertainty of wind speed and solar radiation, *Neural Comput. Appl.* 34 (2022) 10655–10689, <https://doi.org/10.1007/s00521-022-07000-2>.
- [9] J. Dong, P. Li, K. Zhang, W. Ren, P. He, M. Cao, Multi-objective-constraint optimal model for wind-hydro-thermal power joint scheduling based on symbiotic organisms search algorithm, *International Transactions on Electrical Energy Systems* 31 (2021), <https://doi.org/10.1002/2050-7038.12841>.
- [10] M. Mohamed, A.-R. Youssef, S. Kamel, M. Ebeed, E.E. Elattar, Optimal scheduling of hydro-thermal-wind-photovoltaic generation using lightning attachment procedure optimizer, *Sustainability* 13 (2021) 8846, <https://doi.org/10.3390/su13168846>.
- [11] J.D. Hunt, B. Zakeri, A. Nascimento, R. Brandão, Pumped hydro storage (PHS), in: *Storing Energy*, Elsevier, 2022, pp. 37–65, <https://doi.org/10.1016/B978-0-12-824510-1.00008-8>.
- [12] S. Ali, R.A. Stewart, O. Sahin, Drivers and barriers to the deployment of pumped hydro energy storage applications: systematic literature review, *Clean Eng Technol* 5 (2021) 100281, <https://doi.org/10.1016/j.clet.2021.100281>.
- [13] F. Posso Rivera, J. Zalamea, J.L. Espinoza, L.G. Gonzalez, Sustainable use of spilled turbinable energy in Ecuador: three different energy storage systems, *Renew. Sustain. Energy Rev.* 156 (2022) 112005, <https://doi.org/10.1016/j.rser.2021.112005>.
- [14] A.J., B.F.W., G.B. Sheblé, Wood, Power Generation, Operation, and Control, John Wiley & Sons, 2013.
- [15] S.K. Khandualo, A.K. Barisal, P.K. Hota, Scheduling of pumped storage hydrothermal system with evolutionary programming, *Journal of Clean Energy Technologies* (2013) 308–312, <https://doi.org/10.7763/JOET.2013.V1.70>.
- [16] M.S. Fakhar, S.A. Rehman Kashif, M.A. Saqib, F. Mehmood, H.Z. Hussain, Non-cascaded short-term pumped-storage hydro-thermal scheduling using accelerated particle swarm optimization, in: 2018 International Conference on Electrical Engineering (ICEE), IEEE, 2018, pp. 1–5, <https://doi.org/10.1109/ICEE.2018.8566884>.
- [17] P.F. Correia, J.M. Ferreira de Jesus, J.M. Lemos, Sizing of a pumped storage power plant in S. Miguel, Azores, using stochastic optimization, *Elec. Power Syst. Res.* 112 (2014) 20–26, <https://doi.org/10.1016/j.epsr.2014.02.025>.
- [18] A. Karimi, S.L. Heydari, F. Kouchakmohseni, M. Naghilo, Scheduling and value of pumped storage hydropower plant in Iran power grid based on fuel-saving in thermal units, *J. Energy Storage* 24 (2019) 100753, <https://doi.org/10.1016/j.est.2019.04.027>.
- [19] X. Xu, W. Hu, D. Cao, Q. Huang, C. Chen, Z. Chen, Optimized sizing of a standalone PV-wind-hydropower station with pumped-storage installation hybrid energy system, *Renew. Energy* 147 (2020) 1418–1431, <https://doi.org/10.1016/j.renene.2019.09.099>.
- [20] R. Gao, F. Wu, Q. Zou, J. Chen, Optimal dispatching of wind-PV-mine pumped storage power station: a case study in Lingxin Coal Mine in Ningxia Province, China, *Energy* 243 (2022) 123061, <https://doi.org/10.1016/j.energy.2021.123061>.
- [21] J.I. Pérez-Díaz, J. Jiménez, Contribution of a pumped-storage hydropower plant to reduce the scheduling costs of an isolated power system with high wind power penetration, *Energy* 109 (2016) 92–104, <https://doi.org/10.1016/j.energy.2016.04.014>.
- [22] E. Ercan, E. Kentel, Optimum daily operation of a wind-hydro hybrid system, *J. Energy Storage* 50 (2022) 104540, <https://doi.org/10.1016/j.est.2022.104540>.
- [23] A.B. Awan, M. Zubair, G.A.S. Sidhu, A.R. Bhatti, A.G. Abo-Khalil, Performance analysis of various hybrid renewable energy systems using battery, hydrogen, and pumped hydro-based storage units, *Int. J. Energy Res.* 43 (2019) 6296–6321, <https://doi.org/10.1002/er.4343>.
- [24] A.A. Salimi, A. Karimi, Y. Noorizadeh, Simultaneous operation of wind and pumped storage hydropower plants in a linearized security-constrained unit commitment model for high wind energy penetration, *J. Energy Storage* 22 (2019) 318–330, <https://doi.org/10.1016/j.est.2019.02.026>.
- [25] M. Daneshvar, B. Mohammadi-Ivatloo, K. Zare, S. Asadi, Two-stage stochastic programming model for optimal scheduling of the wind-thermal-hydropower-pumped storage system considering the flexibility assessment, *Energy* 193 (2020) 116657, <https://doi.org/10.1016/j.energy.2019.116657>.
- [26] Z. Wang, G. Fang, X. Wen, Q. Tan, P. Zhang, Z. Liu, Coordinated operation of conventional hydropower plants as hybrid pumped storage hydropower with wind and photovoltaic plants, *Energy Convers. Manag.* 277 (2023) 116654, <https://doi.org/10.1016/j.enconman.2022.116654>.
- [27] A. Bhimaraju, A. Mahesh, J.S. Nirbheram, Feasibility study of solar photovoltaic/grid-connected hybrid renewable energy system with pumped storage hydropower system using abandoned open cast coal mine: a case study in India, *J. Energy Storage* 72 (2023) 108206, <https://doi.org/10.1016/j.est.2023.108206>.
- [28] S. Kaur, L.K. Awasthi, A.L. Sangal, G. Dhiman, Tunicate Swarm Algorithm: a new bio-inspired based metaheuristic paradigm for global optimization, *Eng. Appl. Artif. Intell.* 90 (2020) 103541, <https://doi.org/10.1016/j.engappai.2020.103541>.
- [29] M. Dehghani, Š. Hubálovský, P. Trojovský, A new optimization algorithm based on average and subtraction of the best and worst members of the population for solving various optimization problems, *PeerJ Comput. Sci.* 8 (2022) e910, <https://doi.org/10.7717/peerj-cs.910>.
- [30] J.-S. Chou, D.-N. Truong, A novel metaheuristic optimizer inspired by behavior of jellyfish in ocean, *Appl. Math. Comput.* 389 (2021) 125535, <https://doi.org/10.1016/j.amc.2020.125535>.
- [31] M. Dehghani, S. Hubalovsky, P. Trojovsky, Northern goshawk optimization: a new swarm-based algorithm for solving optimization problems, *IEEE Access* 9 (2021) 162059–162080, <https://doi.org/10.1109/ACCESS.2021.3133286>.
- [32] W. Zhao, L. Wang, S. Mirjalili, Artificial hummingbird algorithm: a new bio-inspired optimizer with its engineering applications, *Comput. Methods Appl. Mech. Eng.* 388 (2022) 114194, <https://doi.org/10.1016/j.cma.2021.114194>.
- [33] TummalaS.L.V. Ayyarao, N.S.S. Ramakrishna, R.M. Elavarasan, N. Polumahanthi, M. Rambabu, G. Saini, B. Khan, B. Alatas, War strategy optimization algorithm: a new effective metaheuristic algorithm for global optimization, *IEEE Access* 10 (2022) 25073–25105, <https://doi.org/10.1109/ACCESS.2022.3153493>.
- [34] G. Dhiman, A. Kaur, Spotted Hyena optimizer for solving engineering design problems, in: 2017 International Conference on Machine Learning and Data Science (MLDS), IEEE, 2017, pp. 114–119, <https://doi.org/10.1109/MLDS.2017.5>.
- [35] S. Mirjalili, S.M. Mirjalili, A. Lewis, Grey Wolf optimizer, *Adv. Eng. Software* 69 (2014) 46–61, <https://doi.org/10.1016/j.advengsoft.2013.12.007>.
- [36] S. Mirjalili, SCA: a Sine Cosine Algorithm for solving optimization problems, *Knowl. Base Syst.* 96 (2016) 120–133, <https://doi.org/10.1016/j.knsys.2015.12.022>.
- [37] E. Rashedi, H. Nezamabadi-pour, S. Saryzadi, GSA: a gravitational search algorithm, *Inf. Sci.* 179 (2009) 2232–2248, <https://doi.org/10.1016/j.ins.2009.03.004>.
- [38] G. Dhiman, V. Kumar, Emperor penguin optimizer: a bio-inspired algorithm for engineering problems, *Knowl. Base Syst.* 159 (2018) 20–50, <https://doi.org/10.1016/j.knsys.2018.06.001>.
- [39] S. Mirjalili, A. Lewis, The Whale optimization algorithm, *Adv. Eng. Software* 95 (2016) 51–67, <https://doi.org/10.1016/j.advengsoft.2016.01.008>.
- [40] M.S. Kiran, TSA: Tree-seed algorithm for continuous optimization, *Expert Syst. Appl.* 42 (2015) 6686–6698, <https://doi.org/10.1016/j.eswa.2015.04.055>.
- [41] M.-Y. Cheng, D. Prayogo, Symbiotic Organisms Search: a new metaheuristic optimization algorithm, *Comput. Struct.* 139 (2014) 98–112, <https://doi.org/10.1016/j.compstruc.2014.03.007>.
- [42] R.V. Rao, V.J. Savsani, D.P. Vakharia, Teaching–learning-based optimization: a novel method for constrained mechanical design optimization problems, *Comput. Aided Des.* 43 (2011) 303–315, <https://doi.org/10.1016/j.cad.2010.12.015>.
- [43] X.-S. Yang, Firefly Algorithms for Multimodal Optimization, 2009, pp. 169–178, https://doi.org/10.1007/978-3-642-04944-6_14.
- [44] D. Karaboga, B. Basturk, A powerful and efficient algorithm for numerical function optimization: artificial bee colony (ABC) algorithm, *J. Global Optim.* 39 (2007) 459–471, <https://doi.org/10.1007/s10898-007-9149-x>.

- [45] T.T. Nguyen, D.N. Vo, The application of an effective cuckoo search algorithm for optimal scheduling of hydrothermal system considering transmission constraints, *Neural Comput. Appl.* 31 (2019) 4231–4252, <https://doi.org/10.1007/s00521-018-3356-x>.
- [46] P.T. Ha, D.T. Tran, T.T. Nguyen, Electricity generation cost reduction for hydrothermal systems with the presence of pumped storage hydroelectric plants, *Neural Comput. Appl.* 34 (2022) 9931–9953, <https://doi.org/10.1007/s00521-022-06977-0>.
- [47] C. Wang, S. Chen, Planning of cascade hydropower stations with the consideration of long-term operations under uncertainties, *Complexity* 2019 (2019) 1–23, <https://doi.org/10.1155/2019/1534598>.
- [48] Z. Sun, J. Wang, S. Cheng, H. Luo, G. Zhang, T. Huang, Hierarchical scheduling control method for cascade hydro-PV-pumped storage generation system, *International Transactions on Electrical Energy Systems* 2022 (2022) 1–17, <https://doi.org/10.1155/2022/7382210>.
- [49] G. Liu, G. Ma, W. Huang, S. Chen, Long-term bidding scheduling of a price-maker cascade hydropower station based on supply function equilibrium, *Math. Probl Eng.* 2022 (2022) 1–12, <https://doi.org/10.1155/2022/4710868>.
- [50] F. Yao, Z.Y. Dong, K. Meng, Z. Xu, H.H.-C. lu, K.P. Wong, Quantum-Inspired particle swarm optimization for power system operations considering wind power uncertainty and carbon tax in Australia, *IEEE Trans. Ind. Inf.* 8 (2012) 880–888, <https://doi.org/10.1109/TII.2012.2210431>.
- [51] W.A. Augusteen, S. Geetha, R. Rengaraj, Economic dispatch incorporation solar energy using particle swarm optimization, in: 2016 3rd International Conference on Electrical Energy Systems (ICEES), IEEE, 2016, pp. 67–73, <https://doi.org/10.1109/ICEES.2016.7510618>.
- [52] S. Gao, Y. Gao, Y. Zhang, L. Xu, Multi-strategy adaptive cuckoo search algorithm, *IEEE Access* 7 (2019) 137642–137655, <https://doi.org/10.1109/ACCESS.2019.2916568>.
- [53] C. Li, H. Guo, Y. Zhang, S. Deng, Y. Wang, An improved differential evolution algorithm for a multicommodity location-inventory problem with false failure returns, *Complexity* 2018 (2018) 1–13, <https://doi.org/10.1155/2018/1967398>.
- [54] H. Zhang, D. Yue, X. Xie, C. Dou, F. Sun, Gradient decent based multi-objective cultural differential evolution for short-term hydrothermal optimal scheduling of economic emission with integrating wind power and photovoltaic power, *Energy* 122 (2017) 748–766, <https://doi.org/10.1016/j.energy.2017.01.083>.